

NUCLEAR ENHANCEMENT OF THE PHOTON YIELD IN COSMIC RAY INTERACTIONS

MICHAEL KACHELRIESS¹, IGOR V. MOSKALENKO² AND SERGEY S. OSTAPCHENKO^{2,3}

¹Institutt for fysikk, NTNU, 7491 Trondheim, Norway

²Hansen Experimental Physics Laboratory & Kavli Institute for Particle Astrophysics and Cosmology, Stanford University, Stanford, CA 94305, U.S.A and

³Skobel'syn Institute of Nuclear Physics, Moscow State University, 119991 Moscow, Russia

Draft version October 15, 2018

ABSTRACT

The concept of the nuclear enhancement factor has been used since the beginning of γ -ray astronomy. It provides a simple and convenient way to account for the contribution of nuclei ($A > 1$) in cosmic rays (CRs) and in the interstellar medium (ISM) to the diffuse γ -ray emission. An accurate treatment of the dominant emission process, such as hadronic interactions of CRs with the ISM, enables one to study CR acceleration processes, CR propagation in the ISM, and provides a reliable background model for searches of new phenomena. The *Fermi* Large Area Telescope (*Fermi*-LAT) launched in 2008 provides excellent quality data in a wide energy range 30 MeV – 1 TeV where the diffuse emission accounts for the majority of photons. Exploiting its data to the fullest requires a new study of the processes of γ -ray production in hadronic interactions. In this paper we point out that several commonly used studies of the nuclear enhancement factor miss to account for the spectrally averaged energy loss fraction which ensures that the energy fraction transferred to photons is averaged properly with the spectra of CR species. We present a new calculation of the spectrally averaged energy loss fraction and the nuclear enhancement factor using the QGSJET-II-04 and EPOS-LHC interaction models.

Subject headings: cosmic rays – diffuse radiation – gamma rays: observations

1. INTRODUCTION

Launched in 2008, the γ -ray telescope *Fermi*-LAT provides excellent statistics together with superior angular and energy resolution in a wide energy range from 30 MeV – 1 TeV (Atwood et al. 2009). This energy range is dominated by the diffuse Galactic emission, which is the brightest source on the γ -ray sky. Studies of the diffuse γ -ray emission and extended sources provide invaluable information about CR intensities and spectra in distant locations. Understanding the diffuse emission enables us to study particle acceleration processes, CR propagation in the ISM, and disentangle new phenomena and/or exotic signals (Strong et al. 2007; Su et al. 2010; Ackermann et al. 2012).

The continuous γ -ray emission is generated mainly through the decay of neutral pions and kaons produced in hadronic CR interactions with the ISM, inverse Compton scattering of CR electrons off interstellar photons, and bremsstrahlung. The nuclear component of CRs is dominated by protons, but heavier nuclei also provide an essential contribution to the γ -ray yield. The latter depends on the energy range and on the spectra of the CR species. However, CR spectra and abundances could vary in different locations making an accurate evaluation of their contribution to the γ -ray yield rather difficult.

In all studies of the diffuse γ -ray emission, the effects of heavier nuclei ($A > 1$) in CRs and in the target material are usually taken into account by simply rescaling the γ -ray yield from pp -interactions to the CR-ISM γ -ray yield with a so-called nuclear enhancement factor ε_M . While such a rescaling is a convenient approximation, application of a single enhancement factor in many cases could result in significant errors. In fact, there is no a universal enhancement factor as the rescaling factor depends on the abundances of CRs and the ISM, on the individual spectral shapes of CR species, as well as on the kinematics of the processes involved, e.g., pA vs. Ap yields.

γ -ray production in pp -interactions has been studied in

the past using model fits to the data (Stecker 1973, 1989; Stephens & Badhwar 1981; Dermer 1986a,b), and Monte Carlo simulations (Mori 1997, 2009; Kamae et al. 2006; Kachelrieß & Ostapchenko 2012). The values of the nuclear enhancement factor derived by different authors vary from 1.45 – 2.0, due to the differences in the description of pp -interactions, nuclei abundances, and the scaling formalism. The dependence of ε_M on the spectral shapes of CR species was always neglected, except for a trivial dependence on the relative abundances of CR nuclei. Since the γ -ray data become rather accurate, a new study of the nuclear enhancement factor is warranted.

In this work we study how the spectral shape of the CR species and the kinematics of the processes affect ε_M . We use the QGSJET-II-04 event generator, which accurately reproduces accelerator data (Ostapchenko 2011), to simulate pp -, pA -, and AA -interactions, and compare the results with the most recent calculation by Mori (2009) and with another event generator EPOS-LHC (Pierog et al. 2013) tuned to LHC data.

2. NUCLEAR ENHANCEMENT FACTOR

The photon yield $q_\gamma^{ij}(E_\gamma)$ from scattering of CR species of type i with differential intensity¹ $I_i(E)$ on a target of type j of density n_j is given by

$$q_\gamma^{ij}(E_\gamma) = n_j \int_{E_\gamma}^{\infty} dE \frac{d\sigma^{ij \rightarrow \gamma}(E, E_\gamma)}{dE_\gamma} I_i(E), \quad (1)$$

where $d\sigma^{ij \rightarrow \gamma}(E, E_\gamma)/dE_\gamma$ is the differential inclusive cross section for photon production. For a power-law spectrum, $I_i(E) = K_i E^{-\alpha_i}$, introducing the energy fraction taken by gammas, $z = E_\gamma/E$, and the spectrally averaged moment

$$Z_\gamma^{ij}(E_\gamma, \alpha) = \int_0^1 dz z^{\alpha-1} \frac{d\sigma^{ij \rightarrow \gamma}(E_\gamma/z, z)}{dz}, \quad (2)$$

¹ Throughout the paper, E denotes the energy per nucleon.

we can rewrite the photon yield from channel ij as

$$q_\gamma^{ij}(E_\gamma) = n_j I_i(E_\gamma) Z_\gamma^{ij}(E_\gamma, \alpha_i). \quad (3)$$

Note that in Eq. (3) we evaluate the CR intensity $I_i(E)$ at the photon energy E_γ .

To compare with the most recent approach of Mori (2009), we can factorize out the inelastic cross section $\sigma_{\text{inel}}^{ij}(E)$ and the photon multiplicity $N_\gamma^{ij}(E)$ from the definition of the moment, i.e., we define²

$$\tilde{Z}_\gamma^{ij}(E_\gamma, \alpha) = \frac{Z_\gamma^{ij}(E_\gamma, \alpha)}{\sigma_{\text{inel}}^{ij}(E_\gamma) N_\gamma^{ij}(E_\gamma)}, \quad (4)$$

with

$$N_\gamma^{ij}(E) = \int_0^1 dz f_{ij \rightarrow \gamma}(E, z). \quad (5)$$

Here we introduced also the normalized (per inelastic event) photon energy distribution

$$f_{ij \rightarrow \gamma}(E, z) = \frac{1}{\sigma_{\text{inel}}^{ij}(E)} \frac{d\sigma^{ij \rightarrow \gamma}(E, z)}{dz}. \quad (6)$$

If the inclusive photon cross section satisfied Feynman scaling,

$$\frac{d\sigma^{ij \rightarrow \gamma}(E, z)}{dz} = F(z), \quad (7)$$

$\tilde{Z}^{ij} = 1$ would hold for the particular case $\alpha = 1$; on the other hand, for $\alpha = 2$, \tilde{Z}^{ij} would correspond to the average energy fraction taken by a produced photon (c.f. Eqs. [2], [4-7]).

We can now rewrite the photon yield from a channel ij as

$$q_\gamma^{ij}(E_\gamma) = n_j I_i(E_\gamma) \sigma_{\text{inel}}^{ij}(E_\gamma) N_\gamma^{ij}(E_\gamma) \tilde{Z}_\gamma^{ij}(E_\gamma, \alpha_i). \quad (8)$$

It is easy to see from Eq. (8) that the photon yield is not just proportional to the inelastic cross section $\sigma_{\text{inel}}^{ij}(E)$ and the number $N_\gamma^{ij}(E)$ of photons produced per interaction, but depends rather on the spectrally averaged energy fraction transferred to photons – via the “Z-factors” defined in Eqs. (2) and (4). Thus, the yield generally depends on both, the production spectrum of photons from a channel ij and the spectrum of CR species $I_i(E) \propto E^{-\alpha_i}$, – the steeper is the spectrum and the smaller is the average energy fraction $\langle z \rangle$ transferred to photons, the smaller is $\tilde{Z}_\gamma^{ij}(E_\gamma, \alpha_i)$ and thus the photon yield.

The nuclear enhancement factor ε_M due to the admixture of nuclei in CRs and in the ISM is determined by

$$\begin{aligned} \varepsilon_M &= 1 + \sum_{i+j>2} \varepsilon_{ij} = 1 + \sum_{i+j>2} \frac{n_j I_i(E_\gamma) Z_\gamma^{ij}(E_\gamma, \alpha_i)}{n_p I_p(E_\gamma) Z_\gamma^{pp}(E_\gamma, \alpha_p)} \\ &= 1 + \sum_{i+j>2} \frac{n_j I_i(E_\gamma)}{n_p I_p(E_\gamma)} \frac{\sigma_{\text{inel}}^{ij}}{\sigma_{\text{inel}}^{pp}} \frac{N_\gamma^{ij}}{N_\gamma^{pp}} \frac{\tilde{Z}_\gamma^{ij}(E_\gamma, \alpha_i)}{\tilde{Z}_\gamma^{pp}(E_\gamma, \alpha_p)} \\ &= 1 + \sum_{i+j>2} \frac{n_j I_i(E_\gamma)}{n_p I_p(E_\gamma)} m_{ij}^\gamma(E_\gamma) C_{ij}(E_\gamma, \alpha_i, \alpha_p), \end{aligned} \quad (9)$$

where we introduced also the individual contributions $\varepsilon_{ij}(E_\gamma) = q_\gamma^{ij}(E_\gamma)/q_\gamma^{pp}(E_\gamma)$ of each channel to ε_M , the ratio

² Where we also formally use $E = E_\gamma$.

of inelastic cross sections and multiplicities

$$m_{ij}^\gamma(E) = \frac{\sigma_{\text{inel}}^{ij}(E) N_\gamma^{ij}(E)}{\sigma_{\text{inel}}^{pp}(E) N_\gamma^{pp}(E)}, \quad (10)$$

and the ratio of the Z-factors $C_{ij}(E_\gamma, \alpha_i, \alpha_p) = \tilde{Z}_\gamma^{ij}(E_\gamma, \alpha_i)/\tilde{Z}_\gamma^{pp}(E_\gamma, \alpha_p)$. Note that the correction factors C_{ij} which depend both on the energy distribution of the produced photons and on the slopes of the primary CR spectra were missing in the definition of ε_M used by Mori (2009). As a consequence, the contributions of CR nuclei with $A > 1$ to the nuclear enhancement factor should deviate from the results obtained in that study. Indeed, as noticed above, the correction factors C_{ij} disappear from Eq. (9) only for the (unrealistic) assumption of the validity of Feynman scaling and for the (impractical) case of $\alpha = 1$. On the other hand, for steeply falling spectra, such as in the case of Galactic CRs, $\alpha \gg 1$, the region of large z gives the dominant contribution to the integral defining $\tilde{Z}_\gamma^{ij}(E_\gamma, \alpha)$, i.e. it is the photon spectral shape in the very forward direction, rather than the photon multiplicity N_γ^{ij} , which dominates Z_γ^{ij} .

To illustrate the latter point, let us compare the factors $m_{ij}^\gamma(E)$ (Eq. [10]) and the ratios $Z_\gamma^{ij}(E_\gamma, \alpha)/Z_\gamma^{pp}(E_\gamma, \alpha)$ for $\alpha \gg 1$, for the cases of nucleus-proton ($j = p$) and proton-nucleus ($i = p$) interactions. While $m_{pj}^\gamma = m_{jp}^\gamma$ by virtue of the Lorentz invariance, the behavior of Z_γ^{ip} can be understood from the well-known relation (see Białas et al. 1976) for the mean number of interacting (“wounded”) projectile nucleons $\langle n_{\text{w.p.}}^{ij} \rangle$ in nucleus-nucleus collisions

$$\langle n_{\text{w.p.}}^{ij}(E) \rangle = \frac{i \sigma_{\text{inel}}^{pj}(E)}{\sigma_{\text{inel}}^{ij}(E)}, \quad (11)$$

which holds both in the Glauber approach and in the Reggeon Field Theory, if one neglects the contribution of target diffraction, as demonstrated by Kalmykov & Ostapchenko (1993). This leads, in turn, to an approximate superposition picture for the forward ($z \rightarrow 1$) spectra of secondary photons,

$$\begin{aligned} \frac{d\sigma^{ij \rightarrow \gamma}(E, z)}{dz} &= \sigma_{\text{inel}}^{ij}(E) f_{ij \rightarrow \gamma}(E, z) \\ &\xrightarrow{z \rightarrow 1} \sigma_{\text{inel}}^{ij}(E) \left[\langle n_{\text{w.p.}}^{ij}(E) \rangle f_{pj \rightarrow \gamma}(E, z) \right] \\ &= i \frac{d\sigma^{pj \rightarrow \gamma}(E, z)}{dz}, \end{aligned} \quad (12)$$

which thus gives $Z_\gamma^{jp}/Z_\gamma^{pp} \simeq j > m_{pj}^\gamma$ for $\alpha_j = \alpha_p = \alpha \gg 1$ (c.f. Eq. [2]). On the other hand, assuming that in proton-nucleus and proton-proton interactions the shapes of the photon production spectra are similar in the forward direction, i.e. $f_{pj \rightarrow \gamma}(E, z) \simeq f_{pp \rightarrow \gamma}(E, z)$ at large z , one obtains³

$$\frac{Z_\gamma^{pj}}{Z_\gamma^{pp}} \simeq \frac{\sigma_{\text{inel}}^{pj}}{\sigma_{\text{inel}}^{pp}} < m_{pj}^\gamma. \quad (13)$$

Thus, CR nuclei generally provide a larger contribution to the nuclear enhancement factor ε_M , compared to previous calculations based on m_{ij}^γ , while the opposite is true for the contribution of nuclear species from the ISM.

³ In reality, $f_{pj \rightarrow \gamma}(E, z)$ becomes smaller than $f_{pp \rightarrow \gamma}(E, z)$ at $z \rightarrow 1$, which may lead to a further decrease for the ratio $Z_\gamma^{pj}/Z_\gamma^{pp}$ in the large α limit, compared to Eq. (13), though precise results are model-dependent (see the discussion by Kachelrieß & Ostapchenko 2012).

3. NUMERICAL RESULTS

The normalized Z -factors $\tilde{Z}_{\gamma}^{ij}(E_{\gamma}, \alpha)$ were calculated using the QGSJET-II-04 model by Ostapchenko (2011). Table 1 compares the dependence of $\tilde{Z}_{\gamma}^{ij}(E_{\gamma}, \alpha)$ on the CR spectral index α for different production channels $ij \rightarrow \gamma$ for two photon energies $E_{\gamma} = 10$ and 100 GeV. Note that \tilde{Z}_{γ}^{ij} (c.f. Eq. [4]) specifies the difference between the factor $Z_{\gamma}^{ij}(E_{\gamma}, \alpha)$, which defines the partial photon yield from the channel $ij \rightarrow \gamma$, and the product $\sigma_{\text{inel}}^{ij}(E_{\gamma}) N_{\gamma}^{ij}(E_{\gamma})$.

It is clear that \tilde{Z}_{γ}^{ij} decreases strongly for steeper spectral slopes. This is not surprising since the ratio $Z_{\gamma}^{ij}(E_{\gamma}, \alpha)/\sigma_{\text{inel}}^{ij}(E_{\gamma})$ corresponds to a spectrally averaged fraction of the primary energy, $z = E_{\gamma}/E$, taken by the produced photons, rather than to the photon multiplicity – the steeper is the spectral slope the smaller part of the very forward production spectrum of photons $f_{ij \rightarrow \gamma}(z)$ contributes to the integral in Eq. (2). This explains also why \tilde{Z}_{γ}^{ij} decreases with energy, especially for large α . For relatively small α , the integral in Eq. (2) receives a noticeable contribution from the region of small z , which corresponds to the central rapidity plateau in the center-of-mass frame for the given process and which is responsible for the rise of the photon multiplicity $N_{\gamma}^{ij}(E)$ with energy due to the violation of Feynman scaling for $f_{ij \rightarrow \gamma}(E, z)$ at small z . However, for large α the ratio $Z_{\gamma}^{ij}(E_{\gamma}, \alpha)/\sigma_{\text{inel}}^{ij}(E_{\gamma})$ is governed by the energy dependence of the production spectrum $f_{ij \rightarrow \gamma}(E, z)$ at $z \rightarrow 1$, which satisfies approximately Feynman scaling. For $\alpha \gg 1$ this leads to⁴

$$\frac{\tilde{Z}_{\gamma}^{ij}(E_2, \alpha)}{\tilde{Z}_{\gamma}^{ij}(E_1, \alpha)} \propto \frac{N_{\gamma}^{ij}(E_1)}{N_{\gamma}^{ij}(E_2)}, \quad (14)$$

i.e. $\tilde{Z}_{\gamma}^{ij}(E_{\gamma}, \alpha)$ decreases with energy inversely proportional to the photon multiplicity in the process.

For practical applications, more important are the ratios $Z_{\gamma}^{ij}/Z_{\gamma}^{pp}$ that enter the expressions for the partial contributions ε_{ij} to the nuclear enhancement factor in Eq. (9). The respective results for different production channels and for different spectral indices calculated with QGSJET-II-04 are compiled in Table 2 for $E_{\gamma} = 10$ and 100 GeV; the corresponding ratios m_{ij}^{γ} of inelastic cross sections and multiplicities (Eq. [10]) are also shown for comparison. These results confirm our qualitative expectations from the previous Section – the actual enhancement factor for He+ p collisions, compared to the pp case, is noticeably higher than estimated from $m_{\text{He}p}^{\gamma}$, while for p +He interactions the opposite is true. Obviously, the discussed trends are stronger for steeper CR spectra (larger α) due to the increasing dominance of the very forward part of the photon production spectrum. The same qualitative behavior is observed when comparing the ratios $Z_{\gamma}^{ij}/Z_{\gamma}^{pp}$ and the factors m_{ij}^{γ} , as calculated using the SIBYLL 2.1 (Ahn et al. 2009) and EPOS-LHC (Pierog et al. 2013) models (Table 2), though the numerical results prove to be quite model-dependent⁵.

⁴ To be more precise, Feynman scaling for $f_{ij \rightarrow \gamma}(E, z)$ is (slightly) broken also at $z \rightarrow 1$, with the spectrum becoming somewhat softer at higher energies. This leads to an additional energy decrease of \tilde{Z}_{γ}^{ij} , compared to Eq. (14).

⁵ A detailed comparison of different model predictions for photon production with available accelerator data will be presented elsewhere.

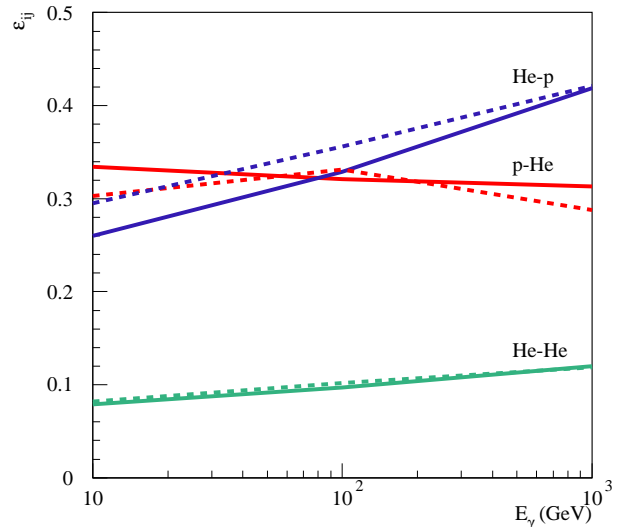


FIG. 1.— Partial contributions ε_{ij} to ε_{M} for several reaction channels, as indicated in the plot, calculated with QGSJET-II-04 (solid lines) and EPOS-LHC (dashed lines) models.

Table 3 shows Z -factors Z_{γ}^{ij} for various channels of photon production in CR interactions. For these calculations we use two up-to-date hadronic interaction models, QGSJET-II-04 and EPOS-LHC. These results can be used for calculations of the nuclear enhancement factor when the combined spectrum of a group of CR nuclei can be approximated by a power-law, $I_i(E) = K_i E^{-\alpha_i}$.

As an illustration, we perform a calculation of ε_{M} in the energy range $E_{\gamma} = 10 - 1000$ GeV, based on Eq. (9), using the high energy limit of the parametrization of the spectra of groups of CR nuclei by Honda et al. (2004); the respective parameters K_i and α_i are given in Table 4 for convenience. The values of ε_{M} are given in Table 5 for the two interaction models. As we already emphasized above, our results for partial contributions to the nuclear enhancement factor from proton-nucleus (ε_{pj}) and nucleus-proton (ε_{ip}) collisions demonstrate important differences from the approach by Mori (2009) and manifest a significant model dependence (c.f. Table 2). However, the respective corrections work in the *opposite directions* and partly compensate each other. As a consequence, our results for ε_{M} in *this particular case*, for both interaction models considered, agree within 5% with those of Mori (2009), who used a different event generator, DPMJET-III.

Fig. 1 shows the energy dependence of the partial contributions ε_{ij} for p +He, He+ p , and He+He channels. It is noteworthy that the smaller index α_{He} of the He component compared to protons has a twofold impact on $\varepsilon_{\text{He}p}$ and $\varepsilon_{\text{HeHe}}$: first, the relative abundance of He increases with energy, and, second, the respective Z -factors become larger for smaller α .

Finally, it is worth stressing that the concept of the nuclear enhancement factor does not work in the case of a sharp change in the CR spectral index, as, e.g., around a spectral break at 230 GV found⁶ in the p and He combined data by ATIC-2 (Panov et al. 2009), CREAM (Yoon et al. 2011), and PAMELA (Adriani et al. 2011). In such a case, a direct convolution of the spectra for different groups of CR nuclei with the respective photon production distributions, as in Eq. (1),

⁶ We note that preliminary results from the AMS-02 experiment (<http://www.ams02.org/2013/07/new-results-from-ams-presented-at-icrc-2013/>), with large statistics, do not show any spectral feature around 230 GV.

is more appropriate. Additionally, if such spectral breaks are observed at different energies per nucleon for different groups of nuclei (e.g., Adriani et al. 2011), which is natural to expect from rigidity-dependent processes of CRs acceleration and propagation, one may expect a strong energy dependence of the resulting enhancement factor.

4. CONCLUSION

The concept of the nuclear enhancement factor ε_M provides a simple and convenient way to account for the contribution of heavier nuclei in CRs and in the ISM to the diffuse γ -ray emission. The latter is comparable to the contribution of protons, the most abundant species in CRs and the ISM. We have shown that the value of the enhancement depends strongly on

the spectral shapes of CR species: not only via the respective energy dependence of the partial abundances of primary nuclei, but also via the spectrally averaged photon energy fraction. It is the latter point which was missed in previous calculations. The provided tables allow a calculation of ε_M for an arbitrary composition of CRs and the ISM for a reasonably wide range of power-law indices. The results for ε_M agree approximately with calculations by Mori (2009) for the same spectra of CR species (Honda et al. 2004), although we found somewhat larger value of ε_M at energies $E_\gamma > 100$ GeV.

IVM and SSO acknowledge support from NASA grants NNX13AC47G and NNX13A092G.

REFERENCES

- Ackermann, M., Ajello, M., Atwood, W. B., et al. 2012, *ApJ*, 750, 3
 Adriani, O., Barbarino, G. C., Bazilevskaia, G. A., et al. 2011, *Science*, 332, 69
 Ahn, E.-J., Engel, R., Gaisser, T. K., Lipari, P., & Stanev, T. 2009, *Phys. Rev. D*, 80, 094003
 Atwood, W. B., Abdo, A. A., Ackermann, M., et al. 2009, *ApJ*, 697, 1071
 Białas, A., Bleszynski, M., & Czyz, W. 1976, *Nucl. Phys. B*, 111, 461
 Dermer, C. D. 1986a, *ApJ*, 307, 47
 —. 1986b, *A&A*, 157, 223
 Honda, M., Kajita, T., Kasahara, K., & Midorikawa, S. 2004, *Phys. Rev. D*, 70, 043008
 Kachelrieß, M., & Ostapchenko, S. 2012, *Phys. Rev. D*, 86, 043004
 Kalmykov, N. N., & Ostapchenko, S. S. 1993, *Physics of Atomic Nuclei*, 56, 346
 Kamae, T., Karlsson, N., Mizuno, T., Abe, T., & Koi, T. 2006, *ApJ*, 647, 692
 Mori, M. 1997, *ApJ*, 478, 225
 —. 2009, *Astroparticle Physics*, 31, 341
 Ostapchenko, S. 2011, *Phys. Rev. D*, 83, 014018
 Panov, A. D., Adams, J. H., Ahn, H. S., et al. 2009, *Bulletin of the Russian Academy of Science, Phys.*, 73, 564
 Pierog, T., Karpenko, I., Katzy, J. M., Yatsenko, E., & Werner, K. 2013, *ArXiv: 1306.0121*
 Stecker, F. W. 1973, *ApJ*, 185, 499
 Stecker, F. W. 1989, in *Cosmic Gamma Rays and Cosmic Neutrinos*, ed. M. M. Shapiro & J. P. Wefel, 85–119
 Stephens, S. A., & Badhwar, G. D. 1981, *Ap&SS*, 76, 213
 Strong, A. W., Moskalenko, I. V., & Ptuskin, V. S. 2007, *Annual Review of Nuclear and Particle Science*, 57, 285
 Su, M., Slatyer, T. R., & Finkbeiner, D. P. 2010, *ApJ*, 724, 1044
 Yoon, Y. S., Ahn, H. S., Allison, P. S., et al. 2011, *ApJ*, 728, 122

TABLE 1
NORMALIZED Z -FACTORS $\tilde{Z}_{\gamma}^{ij}(E_{\gamma}, \alpha)$ CALCULATED WITH QGSJET-II-04

Reaction	$\alpha = 1.5$	$\alpha = 2$	$\alpha = 2.5$	$\alpha = 3$	$\alpha = 3.5$	$\alpha = 4$
$E_{\gamma} = 10$ GeV						
$pp \rightarrow \gamma$	$6.3 \cdot 10^{-1}$	$8.6 \cdot 10^{-2}$	$2.3 \cdot 10^{-2}$	$8.3 \cdot 10^{-3}$	$3.6 \cdot 10^{-3}$	$1.8 \cdot 10^{-3}$
$p\text{He} \rightarrow \gamma$	$6.3 \cdot 10^{-1}$	$8.3 \cdot 10^{-2}$	$2.1 \cdot 10^{-2}$	$7.5 \cdot 10^{-3}$	$3.2 \cdot 10^{-3}$	$1.6 \cdot 10^{-3}$
$\text{He}p \rightarrow \gamma$	$6.7 \cdot 10^{-1}$	$9.4 \cdot 10^{-2}$	$2.5 \cdot 10^{-2}$	$9.3 \cdot 10^{-3}$	$4.1 \cdot 10^{-3}$	$2.1 \cdot 10^{-3}$
$\text{HeHe} \rightarrow \gamma$	$6.8 \cdot 10^{-1}$	$9.0 \cdot 10^{-2}$	$2.3 \cdot 10^{-2}$	$8.4 \cdot 10^{-3}$	$3.6 \cdot 10^{-3}$	$1.8 \cdot 10^{-3}$
$E_{\gamma} = 100$ GeV						
$pp \rightarrow \gamma$	$2.9 \cdot 10^{-1}$	$3.5 \cdot 10^{-2}$	$8.4 \cdot 10^{-3}$	$2.8 \cdot 10^{-3}$	$1.2 \cdot 10^{-3}$	$5.7 \cdot 10^{-4}$
$p\text{He} \rightarrow \gamma$	$2.8 \cdot 10^{-1}$	$3.2 \cdot 10^{-2}$	$7.4 \cdot 10^{-3}$	$2.4 \cdot 10^{-3}$	$1.0 \cdot 10^{-3}$	$4.8 \cdot 10^{-4}$
$\text{He}p \rightarrow \gamma$	$3.0 \cdot 10^{-1}$	$3.7 \cdot 10^{-2}$	$9.0 \cdot 10^{-3}$	$3.0 \cdot 10^{-3}$	$1.3 \cdot 10^{-3}$	$6.2 \cdot 10^{-4}$
$\text{HeHe} \rightarrow \gamma$	$2.9 \cdot 10^{-1}$	$3.4 \cdot 10^{-2}$	$7.9 \cdot 10^{-3}$	$2.6 \cdot 10^{-3}$	$1.1 \cdot 10^{-3}$	$5.1 \cdot 10^{-4}$

TABLE 2
RATIOS $Z_{\gamma}^{ij}/Z_{\gamma}^{pp}$ AND m_{ij}^{γ} FACTORS FOR DIFFERENT PRODUCTION CHANNELS
 $ij \rightarrow \gamma$

Reaction	$Z_{\gamma}^{ij}/Z_{\gamma}^{pp}$						m_{ij}^{γ}
	$\alpha = 1.5$	$\alpha = 2$	$\alpha = 2.5$	$\alpha = 3$	$\alpha = 3.5$	$\alpha = 4$	
QGSJET-II-04: $E_{\gamma} = 10$ GeV							
$p\text{He} \rightarrow \gamma$	3.77	3.61	3.47	3.40	3.36	3.34	3.74
$\text{He}p \rightarrow \gamma$	4.01	4.11	4.15	4.18	4.22	4.27	3.74
$\text{HeHe} \rightarrow \gamma$	14.0	13.5	13.2	13.0	12.8	12.6	12.9
QGSJET-II-04: $E_{\gamma} = 100$ GeV							
$p\text{He} \rightarrow \gamma$	3.72	3.49	3.38	3.31	3.26	3.24	3.85
$\text{He}p \rightarrow \gamma$	4.04	4.10	4.13	4.14	4.15	4.16	3.85
$\text{HeHe} \rightarrow \gamma$	13.8	13.2	12.8	12.5	12.3	12.2	13.7
SIBYLL 2.1: $E_{\gamma} = 100$ GeV							
$p\text{He} \rightarrow \gamma$	3.54	3.21	3.03	2.91	2.83	2.78	3.71
$\text{He}p \rightarrow \gamma$	3.71	3.76	3.77	3.77	3.78	3.79	3.71
$\text{HeHe} \rightarrow \gamma$	11.7	10.7	10.2	9.63	9.35	9.13	12.4
EPOS-LHC: $E_{\gamma} = 100$ GeV							
$p\text{He} \rightarrow \gamma$	3.60	3.57	3.45	3.33	3.24	3.18	4.10
$\text{He}p \rightarrow \gamma$	3.94	4.20	4.45	4.72	4.89	5.12	4.10
$\text{HeHe} \rightarrow \gamma$	13.5	13.7	13.5	13.3	13.2	13.1	14.6

TABLE 3
 Z -FACTORS $Z_{\gamma}^{ij}(E_{\gamma}, \alpha)$ (MBARN) FOR DIFFERENT PRODUCTION CHANNELS $ij \rightarrow \gamma$

Projectile nucleus	Target nucleus	$\alpha = 2$	$\alpha = 2.2$	$\alpha = 2.4$	$\alpha = 2.6$	$\alpha = 2.8$	$\alpha = 3$
QGSJET-II-04: $E_{\gamma} = 10$ GeV							
p ($A=1$)	p	5.45	3.06	1.84	1.17	0.771	0.529
He ($A=4$)	p	22.4	12.6	7.62	4.85	3.22	2.21
CNO ($A=14$)	p	76.8	43.8	26.6	17.1	11.4	7.89
Mg-Si ($A=25$)	p	138	78.9	48.2	31.0	20.7	14.4
Fe ($A=56$)	p	298	171	105	67.2	45.0	31.2
p ($A=1$)	He	19.7	10.9	6.48	4.07	2.68	1.83
He ($A=4$)	He	73.7	41.0	24.4	15.3	10.1	6.86
CNO ($A=14$)	He	271	152	91.2	57.7	38.1	26.1
Mg-Si ($A=25$)	He	473	266	160	101	66.8	45.7
Fe ($A=56$)	He	1010	569	342	216	143	97.5
QGSJET-II-04: $E_{\gamma} = 100$ GeV							
p ($A=1$)	p	5.93	3.20	1.86	1.14	0.736	0.492
He ($A=4$)	p	24.3	13.1	7.65	4.72	3.04	2.04
CNO ($A=14$)	p	83.3	45.4	26.6	16.5	10.7	7.21
Mg-Si ($A=25$)	p	149	81.7	48.0	29.8	19.4	13.1
Fe ($A=56$)	p	330	181	107	66.7	43.4	29.3
p ($A=1$)	He	20.7	11.0	6.33	3.85	2.45	1.63
He ($A=4$)	He	78.1	41.7	23.9	14.6	9.29	6.16
CNO ($A=14$)	He	285	153	88.6	54.3	34.9	23.3
Mg-Si ($A=25$)	He	506	273	159	97.7	63.0	42.2
Fe ($A=56$)	He	1100	596	346	213	137	92.1
QGSJET-II-04: $E_{\gamma} = 1$ TeV							
p ($A=1$)	p	6.85	3.61	2.05	1.24	0.786	0.519
He ($A=4$)	p	28.4	15.0	8.51	5.14	3.26	2.14
CNO ($A=14$)	p	95.6	50.6	28.9	17.6	11.2	7.39
Mg-Si ($A=25$)	p	174	92.4	53.0	32.3	20.6	13.6
Fe ($A=56$)	p	378	202	117	71.3	45.7	30.5
p ($A=1$)	He	23.7	12.2	6.83	4.07	2.56	1.67
He ($A=4$)	He	89.2	46.1	25.8	15.4	9.66	6.31
CNO ($A=14$)	He	321	167	93.5	55.8	35.0	22.9
Mg-Si ($A=25$)	He	567	296	167	100	63.3	41.6
Fe ($A=56$)	He	1260	660	375	226	143	94.6
EPOS-LHC: $E_{\gamma} = 10$ GeV							
p ($A=1$)	p	5.83	3.31	2.00	1.27	0.844	0.578
He ($A=4$)	p	26.0	15.0	9.27	6.00	4.04	2.82
CNO ($A=14$)	p	89.6	52.3	32.4	21.1	14.3	9.99
Mg-Si ($A=25$)	p	156	91.5	57.1	37.4	25.5	18.0
Fe ($A=56$)	p	342	203	128	84.6	58.2	41.4
p ($A=1$)	He	20.7	11.4	6.68	4.12	2.64	1.75
He ($A=4$)	He	82.5	46.3	27.7	17.5	11.5	7.79
CNO ($A=14$)	He	309	175	106	67.7	44.9	30.8
Mg-Si ($A=25$)	He	562	322	196	126	83.7	57.6
Fe ($A=56$)	He	1200	692	424	273	183	128
EPOS-LHC: $E_{\gamma} = 100$ GeV							
p ($A=1$)	p	6.34	3.49	2.06	1.29	0.837	0.564
He ($A=4$)	p	26.6	14.9	9.01	5.75	3.84	2.66
CNO ($A=14$)	p	95.4	54.9	33.8	22.0	15.0	10.6
Mg-Si ($A=25$)	p	167	96.2	59.1	38.3	25.9	18.1
Fe ($A=56$)	p	373	216	134	87.9	60.0	42.4
p ($A=1$)	He	22.6	12.3	7.18	4.44	2.88	1.94
He ($A=4$)	He	86.5	47.2	27.7	17.2	11.2	7.60
CNO ($A=14$)	He	321	177	105	66.3	43.7	29.9
Mg-Si ($A=25$)	He	582	324	193	122	80.2	54.7
Fe ($A=56$)	He	1320	744	449	286	190	130
EPOS-LHC: $E_{\gamma} = 1$ TeV							
p ($A=1$)	p	7.61	4.15	2.45	1.54	1.01	0.693
He ($A=4$)	p	31.1	17.3	10.3	6.51	4.31	2.96
CNO ($A=14$)	p	106	60.2	36.7	23.7	16.0	11.3
Mg-Si ($A=25$)	p	192	110	68.2	44.7	30.6	21.8
Fe ($A=56$)	p	433	253	159	105	73.6	53.1
p ($A=1$)	He	25.3	13.4	7.73	4.71	3.01	2.00
He ($A=4$)	He	98.3	53.1	31.0	19.2	12.5	8.44
CNO ($A=14$)	He	360	197	116	72.7	47.5	32.3
Mg-Si ($A=25$)	He	654	361	214	135	88.7	60.6
Fe ($A=56$)	He	1480	829	498	317	210	145

TABLE 4
SPECTRAL PARAMETERIZATIONS FOR GROUPS OF CR NUCLEI (HONDA ET AL.
2004)

Parameters	Groups of nuclei				
	H ($A=1$)	He ($A=4$)	CNO ($A=14$)	Mg-Si ($A=25$)	Fe ($A=56$)
K	14900	600	33.2	34.2	4.45
α	2.74	2.64	2.60	2.79	2.68

TABLE 5
NUCLEAR ENHANCEMENT FACTORS
 ϵ_M CALCULATED FOR CR
COMPOSITION GIVEN IN TABLE 4

Models	Photon energy, GeV		
	10	100	1000
QGSJET-II-04	1.85	1.95	2.09
EPOS-LHC	1.88	2.02	2.09